

PAPER • OPEN ACCESS

Application of an advanced necking criterion for nonlinear strain paths to a complex sheet metal forming component

To cite this article: Klaus Drotleff and Mathias Liewald 2018 *IOP Conf. Ser.: Mater. Sci. Eng.* **418** 012041

View the [article online](#) for updates and enhancements.

You may also like

- [Time evolution photoluminescence studies of quantum dot doped ferroelectric liquid crystals](#)
A Kumar, S Tripathi, A D Deshmukh et al.
- [Pico-ampere current sensitivity and CdSe quantum dots assembly assisted charge transport in ferroelectric liquid crystal](#)
Dharmendra Pratap Singh, Yahia Boussoualem, Benoit Duponchel et al.
- [Fabrication of vertical alignment in ferroelectric liquid crystals for display application](#)
Hirokazu Furue, Toshiki Horiguchi, Miyuki Yamamichi et al.



ECS
The
Electrochemical
Society
Advancing solid state &
electrochemical science & technology

DISCOVER
how sustainability
intersects with
electrochemistry & solid
state science research

Application of an advanced necking criterion for nonlinear strain paths to a complex sheet metal forming component

Klaus Drotleff, Mathias Liewald

Institute for Metal Forming Technology, University of Stuttgart, Holzgartenstr. 17,
70174 Stuttgart, Germany

klaus.drotleff@ifu.uni-stuttgart.de

Abstract. For meeting time, cost and quality targets in industrial sheet metal forming processes, correct formability prediction in a very early project stage has become a crucial factor. It is well known that the conventional Forming Limit Curve (FLC), which is most commonly used for this purpose, is only valid for linear strain paths. Yet, in most industrial sheet metal components, the occurring strain paths are nonlinear. Due to this fact, most users apply a safety margin of 10 to 20% when using the Forming Limit Diagram for formability prediction resulting in higher process robustness, but also increasing component weight and material costs in production. Reasons for the broad application of the FLC in industry is the simple experimental determination of the curve as well as the easy implementation in finite element post-processing. In this paper, an advanced failure criterion for nonlinear strain paths is presented and applied to a deep drawn door inner part. The investigated deep drawing specimen was manufactured using the aluminium alloy AA6014 T4 and the dual phase steel DP600. The sheet thickness was chosen to be closely to 1.0 mm. The calibration procedure of the criterion for arbitrary sheet materials is based purely on uniaxial tensile test data. Experiments for the calibration of the model as well as the application of the criterion to an experimental stamping part will be explained in the paper. Finally, a comparison of the newly presented model with conventional formability evaluation using standard FLC will be given.

1. Introduction

The design of modern sheet metal components is often very complex and modern high strength steel and aluminium alloys used for these components are often more difficult to form than conventional deep drawing steels. After deep drawing the major part geometry in the first operation, trimming, redrawing and restriking operations are often necessary in order to achieve the desired part geometry. To reduce time to market, engineering and tool manufacturing costs as well as revision cycles in tool try-out, tool designs are usually verified before production by using finite element simulation of the forming. To keep computing costs at an acceptable level, the models used for feasibility estimation usually bear simplifying assumptions. Forming tools are considered to be rigid during the forming process [1], forming behaviour of the blank material is modelled using an extrapolated yield curve from uniaxial tensile test data and friction is described using Coulomb's law, for example. Advanced material models considering the effect of anisotropy as well as several other important effects like kinematic hardening, strain rate dependence or draw bead plastification are necessary for realistic forming simulation [2]. For a correct estimation of feasibility, it is also necessary to have exact knowledge about the onset of localised necking and the beginning of rupture for a given sheet material. Since the 1960s, the forming limit curve (FLC) as proposed by Keeler et al. [3] has become an industry standard for this procedure.



Content from this work may be used under the terms of the [Creative Commons Attribution 3.0 licence](https://creativecommons.org/licenses/by/3.0/). Any further distribution of this work must maintain attribution to the author(s) and the title of the work, journal citation and DOI.

Experiments for measuring critical strain values corresponding to the onset of localised necking have been standardised in ISO 12004-2 [4]. Testing setups as proposed by Nakajima or Marciniak produce idealised strain paths enabling the determination of the onset of localised necking. Strain measurement is usually done using digital image correlation systems. These optical measurement devices also allow the use of advanced time dependent methods for determination of the onset of localised necking.

Since the works of Müschenborn and Sonne [5], it is well known that forming history influences the beginning of localisation in the sheet metal forming process and that the conventional forming limit curve does not take these effects into account. Many advanced models have been presented for improved failure prediction. Generalized Forming Limit Concept (GFLC) by Volk [6–8], Modified Maximum Force Criterion (MMFC) with many different extensions by Hora [9–11] and forming limit stress curves as proposed by Stoughton [12–14] are some of the very well-known approaches for improved prediction of localised necking under arbitrary loading conditions. Thus, increased prediction quality often comes with increased time and characterisation costs. To overcome this problem and to achieve good feasibility prediction with a low number of experiments, a new model based on the approaches presented in [15–17] will be presented in this paper. The model and the calibration procedure are described in the following chapter. Nonlinear strain paths inevitably occur in most sheet metal forming processes. The nonlinearity, which can be described by the change of the ratio of minor to major strain $\beta = \Delta\varphi_2/\Delta\varphi_1$ during the forming process, is usually rather small, being a value of less than 5%. Furthermore, most nonlinear strain paths do not come close to critical strain combinations of the forming material. In these cases, the conventional forming limit curve as described in the ISO standard seems to provide a reasonably good feasibility prediction. In tough cases, however, nonlinear strain paths with stronger nonlinearities and critical strain values do occur during manufacturing of sheet metal components, hence leading to a difficult formability prediction using the conventional FLC.

2. Model for prediction of localised necking for arbitrary strain paths

The model presented in this paper is purely based on tensile test data and a modified version of the FLC calculation approach presented by Abspoel et al. in 2013 [18]. In order to take into account the effect of nonlinear strain paths, additional tensile tests of pre-stretched specimen are conducted. For full calibration of the model, 36 tensile tests according to ISO 6892 [19] are needed. The calibration procedure includes tensile tests in 0°, 45° and 90° to the rolling direction, which are usually conducted during the preparation of material cards for forming simulation anyway. Depending on the maximum uniform elongation of the material, a uniaxial pre-stretching up to 15% effective strain is carried out prior to uniaxial tensile tests to calibrate the model. The pre-stretching is conducted using a conventional uniaxial tensile testing machine with rectangular specimen from which secondary “dog bone” specimen according to ISO 50125 can be prepared for further experiments. In [20] the experimental procedure is described in detail. The experimental setup is summarised in table 1.

Table 1. Overview of number of experiments necessary for calibration of the proposed model.

Amount of pre-stretching [von Mises effective strain]	# of sample geometries
0%	3 for each rolling direction (0°, 45°, 90°)
5%	
10%	
15%	
#Total specimen tested	36

From these tests, a set of material data is determined, especially including strain dependent material parameters like Lankford coefficients (r-values) in three different directions, hardening exponent n , maximum uniform elongation A_g and maximum elongation A_{80} . The tests are carried out using a conventional “dog bone” specimen as described in DIN 50125. Since uniaxial tensile tests in three

different directions are conducted anyway, for the determination of yield locus and yield curve, the number of extra tensile tests required by the proposed model to predict necking for arbitrary strain paths is only 27.

2.1. Setup of the nonlinear FLC criterion

The strain-dependent material parameters determined in the tensile test of pre-stretched specimens show significant dependence on the amount of pre-strain. Based on the methods described in [5,17,21], nonlinear strain paths can be simplified by consecutive linear sections. Combining these linear sections and using the von Mises effective strain as a measure for prior deformation, an improved prediction of material behaviour can be achieved. From [22] and [23] it can be derived, that the hardening exponent, Lankford coefficient and fracture strain have a significant influence on the FLC. Figures 1 and 2 show the change of Lankford coefficient r , hardening exponent n and fracture strain A_{80} for increasing amounts of pre-strain.

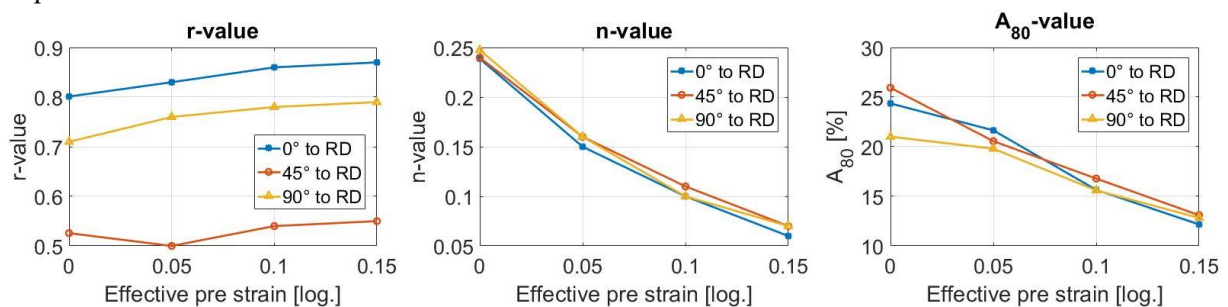


Figure 1. Influence of pre-stretching on resulting Lankford coefficients, hardening exponents and fracture strains of AA6014 T4.

For both materials investigated, the first five percent of pre-stretching is observed to cause an almost common trend of increase in Lankford parameters and reduction of hardening exponent and fracture strains on the other hand. Lankford coefficients, hardening values and fracture strains were determined as described in ISO 6811.

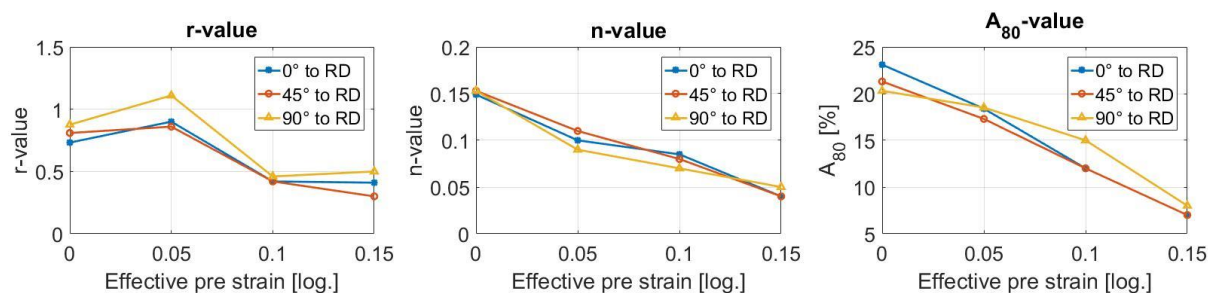


Figure 2. Influence of pre-stretching on resulting Lankford coefficients, hardening exponents and fracture strains of DP600.

Beyond the 5% pre-stretching, figures 1 and 2 demonstrate further dependence but in a different manner based on the investigated material. The complicated trend may originate from the dual-phase nature of DP600. As shown in figures 1 and 2, material properties change significantly within a range of 0 and 10% pre-stretching applied to the tensile test specimens. It is expected that the changes in these strain dependent material parameters are directly influencing the shape and position of the FLC. Based on this observation, the formulations used for calculation of the FLC points by Abspoel et al. [18] have been adapted as shown in table 2. The formulas presented in table 2 can be calculated using fracture strain value A_{80} , r -value in the desired rolling direction of the sheet material, sheet thickness t and hardening exponent n . The prediction of changes in the shape of the FLC is enriched by an additional formula providing a fifth point between the pure uniaxial and the plane-strain point. Since the calculated FLCs are afterwards compared to experimental data from Nakajima-tests, the formulas have been

modified to take the biaxial shift of the plane-strain point into account. The transformation of FLCs with biaxial shift from Nakajima-test to FLCs from the Marciniak-test can be conducted using the methods presented by Leppin et al.[24].

Table 2. Mathematic model used for calculation of FLCs for arbitrary strain paths.

FLC point	Formulation
Uniaxial point	$\varphi_{1UA} = \frac{(1 + 0.787r(\varphi)^{0.701})((0.0626 A_{80}^{0.567} + (t - 1)(0.12 - 0.0024 A_{80}))}{\sqrt{1 + (0.797r(\varphi)^{0.701})^2}}$
	$\varphi_{2UA} = -\frac{(0.626A_{80}^{0.567} + (t - 1)(0.12 - 0.0024A_{80})0.797r(\varphi)^{0.701}}{\sqrt{1 + (0.797r(\varphi)^{0.701})^2}}$
Intermediate uniaxial point	$\varphi_{1IMU} = \frac{(797r(\varphi)^{0.701})((0.0626 A_{80}^{0.567} + (t - 1)(0.12 - 0.0024 A_{80}))}{\sqrt{1 + (0.797r(\varphi)^{0.701})^2}}$
	$\varphi_{2IMU} = -\frac{(0.626A_{80}^{0.567} + (t - 1)(-0.0024A_{80})0.01r(\varphi)^{0.701}}{\sqrt{1 + (0.797r(\varphi)^{0.701})^2}}$
Plane-strain point	$\varphi_{1PS} = 0.0084A_{80} + 0.0017A_{80}(t - 1)$
	$\varphi_{2PS} = 0.0183$
Intermediate biaxial point	$\varphi_{1IM} = 0.0062A_{80} + 0.18 + 0.0027A_{80}(t - 1)$
	$\varphi_{2IM} = 0.75(0.0062A_{80} + 0.18 + 0.0027A_{80}(t - 1))$
Equibiaxial point	$\varphi_{1BA} = \varphi_{2BA} = 0.00215A_{80} + 0.25 + 0.00285A_{80}t$
	$\varphi_{2BA} = 0.00215A_{80} + 0.25 + 0.00285A_{80}t$

Figures 3 and 4 compare the calculated and experimentally determined FLCs for the dual phase steel and the 6014 aluminium alloy respectively. The formulations from table 2 then have been adapted to regard the effect of nonlinear strain paths indirectly defined by changing r-values, hardening exponent and maximum elongation.

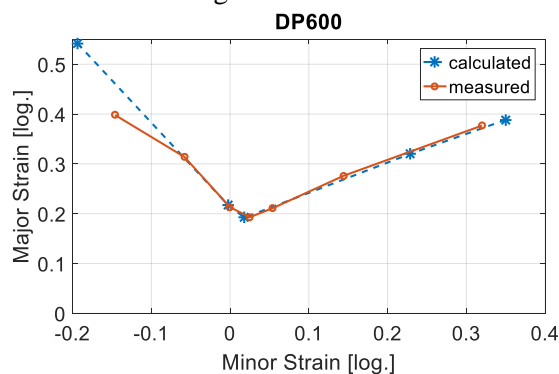


Figure 3. Displacement splines for uniaxial-, plane-strain and biaxial FLC point in comparison to experimental data.

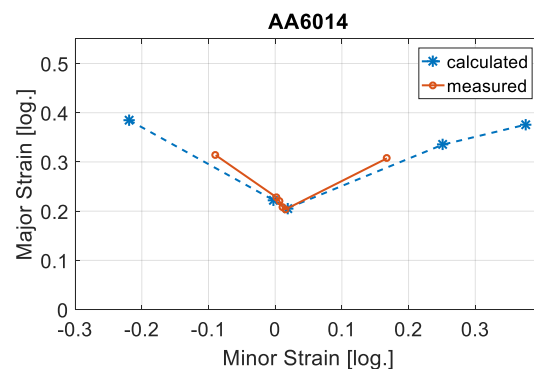


Figure 4. Displacement splines for uniaxial-, plane-strain and biaxial FLC in comparison to experimental data.

For this purpose, parameters A, B, C and D of so-called polynomial displacement functions are fitted to the experimental material data and given in table 3. The mathematical formulation is given in equation

1. Parameter D is chosen to be equal to the major strain value of the standard material without pre-stretching. Using these displacement functions for the uniaxial-, plane-strain and biaxial point, a three-dimensional failure surface is generated to shift the conventional 0-FLC.

$$\varphi_1 = A\varphi_{\text{eff}}^3 + B\varphi_{\text{eff}}^2 + C\varphi_{\text{eff}} + D \quad (1)$$

Table 3. Parameters of calculated displacement functions for uniaxial, plane-strain and biaxial FLC point.

Parameter	Uniaxial point		Plane-strain point		Biaxial point	
	DP600	AA6014	DP600	AA6014	DP600	AA6014
A	-0.009	30.75	-28.61	-37.80	-22.71	0
B	-1.40	-8.16	9.815	14.97	4.908	-1.869
C	-0.649	-0.282	-1.418	-2.044	-0.496	-0.018
D	0.389	0.314	0.195	0.208	0.353	0.307

2.2. Visualisation of the calculated failure surface for arbitrary strain paths

Resulting splines in comparison to experimental data are shown in figures 5 and 6. The shape of the FLC changes with increasing pre-stretching of the material DP600 and AA6014. The FLCs are calculated using the formulations given in table 2 and swept using the displacement function from equation 1. The displacement function is applied only to the major strain values of the formulas for FLC calculation. Major strain values for the five FLC points described in table 2 are therefore calculated according to equation 2.

$$\varphi_{1_{nl}} = \varphi_1 - \left(\varphi_{1PS} - (A\varphi_{\text{eff}}^3 + B\varphi_{\text{eff}}^2 + C\varphi_{\text{eff}} + D) \right) \quad (2)$$

The minor strain values of the five FLC points calculated do not change significantly with increasing amount of pre-strain. During experimental testing, it can be seen that the uniaxial, plane-strain and biaxial points are changing their position with increasing level of pre-stretching.

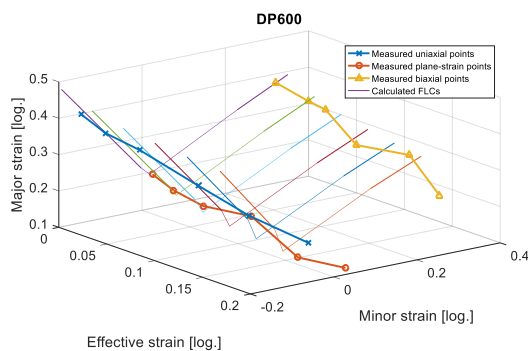


Figure 5. Displacement splines for uniaxial-, plane-strain and biaxial FLC point in comparison to experimental data.

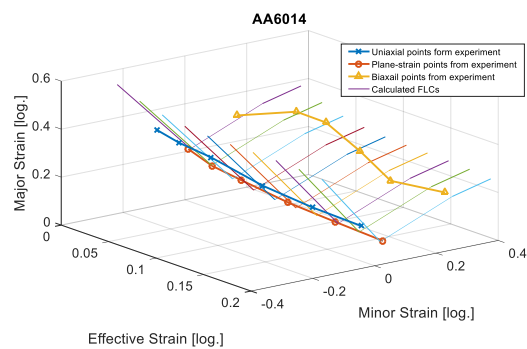


Figure 6. Displacement splines for uniaxial-, plane-strain and biaxial FLC in comparison to experimental data.

3. Application to experimental stamping of a door inner component

After calibration of the model for AA6014 and DP600 materials, a finite element forming simulation for a scaled down version of a door inner component was conducted. Material cards for AA6014 and DP600 with sheet thicknesses of 1.04 mm and 0.98 mm were set up using data from uniaxial tensile tests, bulge tests and FLC data from conventional Nakajima-experiments. The yield curve extrapolation according to Hockett-Sherby [2] was used for both materials. The yield locus of DP600 material was

modelled using Barlat Yld89 [25] function, as given in AutoForm R7. For aluminium alloy AA6014, the BBC yield criterion was applied [2]. The material parameters used in the forming simulation are summed up in the following table 4. The friction coefficient was set to 0.15 and kept constant throughout the forming simulation to resemble commonly used values in industrial application. The blankholder force for DP600 alloy during forming simulation as well as during experimental stamping was chosen to be 750 kN. For the aluminium alloy AA014, a blankholder force of 350 kN was applied. Blank size and position in the drawing tool were the same for both materials. Lubrication of DP600 was chosen to be 4 g/m². The aluminium alloy was formed using pre-lubrication agents applied to the blank.

Table 4. Material parameters used in forming simulation.

Parameter	DP600 – thickness 0.98 mm	AA6014 – thickness 1.04 mm
σ_{sat}	734.3 MPa	308.5 MPa
σ_i	231.9 MPa	120.9 MPa
n	0.198	0.244
r_0	0.732	0.78
r_{45}	0.809	0.49
r_{90}	0.876	0.68

It is well known that different material models have a huge influence on results of forming simulation. Therefore, a simulation study was carried out in order to determine the influence of the yield locus description on resulting formability. The forming simulations were validated by comparing draw-in and sheet thickness in several characteristic points. Since there are about 173000 elements in the forming simulation of the door inner component, the strain linearity function of AutoForm R7 has been applied to determine critical nonlinear strain paths. This is done by checking the β -values of each element during the forming process. If this value is above 0.02, resembling a change in the strain path of more than 10%, the element is marked as nonlinear and the IFU-FLC-Criterion is applied.

Failure prediction was carried out comparatively using conventional FLC according to ISO 12004-2 standard as well as the IFU-FLC-Criterion described in section 2 of this paper. If the conventional FLC according to the ISO standard is applied, the onset of localised necking is predicted in the areas shown in the figures 7 and 8 for the aluminium and the DP alloy. Simulation results along with the nonlinear strain paths are marked with red dots.

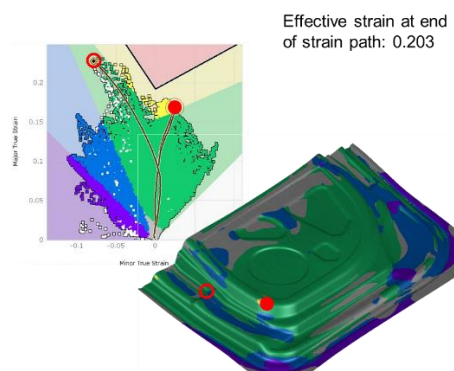


Figure 7. Resulting forming simulation of DP600 alloy and critical necking areas (red dot).

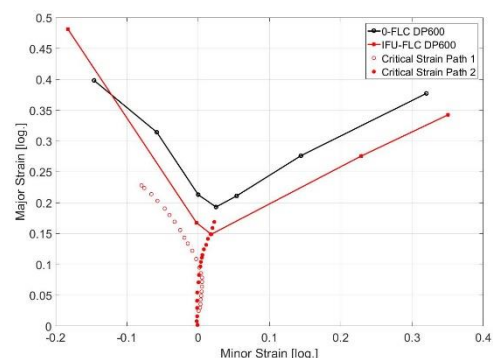


Figure 8. FLD of door inner stamping for DP600 and critical nonlinear strain path marked in red.

From figures 7 and 8, it can be seen that if the conventional FLC is used, risk of necking is predicted in the left radius of the DP600 component (marked with a red dot in figure 7). Using the FLC determined

from IFU-FLC-Criterion as shown in figure 8, the onset of localised necking for this area is predicted about 2 mm before the bottom dead centre. Results of forming simulation of AA6014 alloy are shown in figures 9 and 10. Using standard FLC, the forming simulation of AA6014 only predicts a very small area with risk of necking in the left lower radius of the component at a maximum drawing depth of 95 mm. The IFU-FLC-Criterion on the other hand predicts necking at a drawing depth of 92 mm.

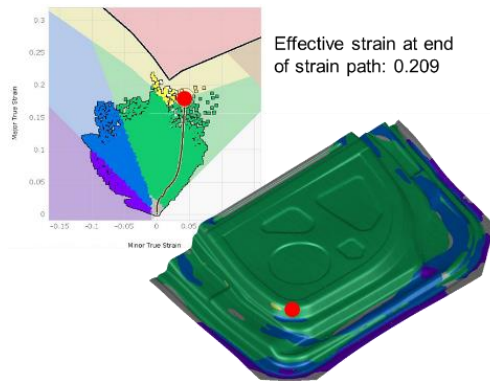


Figure 9. Resulting forming simulation of AA6014 alloy and necking area (red dot).

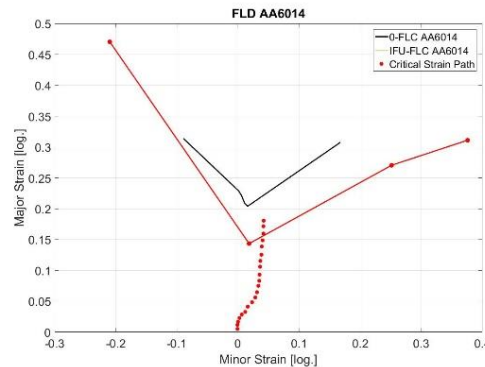


Figure 10. FLD of door inner stamping for AA6014 and critical nonlinear strain path marked in red.

4. Comparison with experimental data

From the experimental forming of the door inner component it becomes obvious that localised necking occurs very closely to the areas predicted by the IFU-FLC-Criterion. In order to compare experimental and simulation results, the drawing depth at the onset of the localised necking, the necking area in the formed component and the draw-in are compared. Table 5 shows pictures of the formed door inner parts made of DP600 and AA6014 alloy. The maximum drawing depth of the component is 95 mm. The failure position of the drawn part was the lower left area independent of the alloy used. The critical drawing depth determined from forming experiments was 94.5 mm for DP600 and 92 mm for AA6014 alloy. In table 6, a comparison of the calculated and experimental critical drawing depth using standard FLC and IFU-FLC-Criterion are given.

Table 5. Experimental results of stamping door inner components with DP600 and AA6014 alloy. Investigated areas marked with red dots and circles.

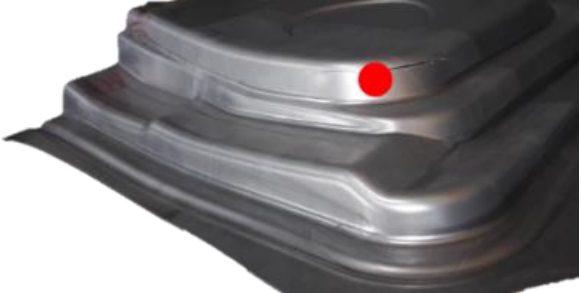
DP600 stamping with necking area	AA6014 stamping with crack in lower left radius
	

Table 6. Comparison of critical drawing depth for the onset of localised necking.

Criterion	DP600 – thickness 0.98 mm	AA6014 – thickness 1.04 mm
Standard FLC	No necking at 95 mm drawing depth	No necking at 95 mm drawing depth
IFU-FLC-Criterion	Necking at 93 mm	Necking at 92 mm
Experiment	Slight necking at 94.5 mm	Fracture at 95 mm

5. Conclusions and outlook

The determination of localised necking in complex sheet metal forming operations is crucial for achieving high process robustness and part quality within constraints of time and cost. In this paper, an advanced failure model for prediction of localised necking for arbitrary strain paths is presented. The model is purely based on data determined in uniaxial tensile tests and can be calibrated for any sheet metal material with only 36 tensile test specimen. The mathematical model presented is capable of predicting five FLC points for onset of localised necking and taking the influence of changing material properties due to pre-stretching into account. In this paper, the presented model is calibrated for the aluminium alloy AA6014 and the dual phase steel alloy DP600. Validation of the presented model is done using an experimental inner door stamping where critical drawing depth at necking and fracture was experimentally determined and compared to predicted critical drawing depths in sheet metal forming simulation. As described in section 4 of this paper, the predicted drawing depths for the steel and aluminium alloy are in good agreement with the experimental results. Using the advanced necking criterion presented in this paper forming simulation can be improved.

In further research projects, the application of the presented criterion to multi step forming operations will be investigated as well as the application of this criterion to further sheet metal materials like conventional deep drawing steels and 5xxx aluminium alloys. The implementation of the presented criterion to commercial finite element forming software can be done very easily due to the fact that the criterion does only need post processing data, which is already calculated by every finite element software.

References

- [1] Roll K 2008 Simulation of sheet metal forming - Necessary developments in the future Numisheet 2008 59–68
- [2] Banabic D 2010 Sheet metal forming processes: Constitutive modelling and numerical simulation (Berlin: Springer)
- [3] Keeler S P 1961 Plastic Instability and fracture in sheets stretched over rigid punches: MIT, D.Sc. thesis, May 1961--Cambridge, 1961 (Cambridge: MIT)
- [4] DIN Deutsches Institut für Normung e.V. Metallische Werkstoffe - Bleche und Bänder - Bestimmung der Grenzformänderungskurve - Teil 2: Bestimmung von Grenzformänderungskurven im Labor (ISO12004-2:2008) 77.040.10
- [5] Müschenborn W and Sonne H-M 1975 Einfluss des Formänderungsweges auf die Grenzformänderungen des Feinblechs Arch. des Eisenhüttenwesens 46 597–602
- [6] Volk W, Böttcher O, Feistle M, Gaber C and Jocham D Advanced Failure Prediction in Sheet Metal Forming Forming Technology Forum 2015 pp 43–7
- [7] Volk W, Hoffmann H, Suh J and Kim J 2012 Failure prediction for nonlinear strain paths in sheet metal forming CIRP Ann. - Manuf. Technol. 61 259–62
- [8] Volk W and Gaber C 2017 ScienceDirect Investigation and Compensation of Biaxial Pre-strain During the Standard Nakajima- and Marciniak-test Using Generalized Forming Limit Concept
- [9] Hora P 2006 Numerical and experimental methods in prediction of forming limits in sheet forming and tube hydroforming processes: FLC-Zurich 06 ; proceedings ; March 15th - 16th

- 2006, Gottlieb Duttweiler Institut, Ruschlikon/Zurich, Switzerland (Zurich: Inst. für Virtuelle Produktion, ETH Zurich)
- [10] Manopulo N, Hora P, Peters P, Gorji M and Barlat F 2015 An extended Modified Maximum Force Criterion for the prediction of localized necking under non-proportional loading *Int. J. Plast.*
- [11] Manopulo N, Peters P and Hora P Prediction of localized necking for nonlinear strain paths using the modified maximum force criterion (MMFC) and the homogeneous anisotropic hardening model (HAH) IDDRG 2013 Conference pp 175–81
- [12] Review D O E M 2012 Non Linear Strain Paths Thomas B . Stoughton Project ID LM064 Timeline Total project funding Project Leads :
- [13] Dick R E, Yoon J W and Stoughton T B 2015 Path-independent forming limit models for multi-stage forming processes *Int. J. Mater. Form.*
- [14] Stoughton T B Verbesserte Beschreibung der Umformgrenzen von Metallen unter nicht-linearen und nicht-ebenen Formänderungspfaden 231–52
- [15] Werber A 2015 Einfluss nicht-linearer Dehnpfade auf Bauteileigenschaften und Versagen von Aluminium-6xxx-Legierungen vol 74(Bonn: Inventum)
- [16] Drotleff K and Liewald M 2017 Novel Approach for Prediction of Localized Necking in Case of Nonlinear Strain Paths *J. Phys. Conf. Ser.* 896 12113
- [17] Liewald M and Drotleff K 2016 Bewerten von Umformgrenzen bei nicht-linearen Beanspruchungen in der Praxis ed Europäische Forschungsgesellschaft für Blechverarbeitung e.V.
- [18] Abspoel M, Scholting M E and Droog J M M 2013 A new method for predicting Forming Limit Curves from mechanical properties *J. Mater. Process. Technol.* 213 759–69
- [19] DIN Deutsches Institut für Normung e.V. 2009 Metallischer Werkstoffe - Zugversuch - Teil 1: Prüfverfahren bei Raumtemperatur
- [20] Drotleff K, Liewald M and Mosebach J-T Improved Failure Criterion for Nonlinear Strain Paths *Forming Technology Forum 2015*
- [21] Drotleff K and Liewald M 2017 Novel Approach for Prediction of Localized Necking in Case of Nonlinear Strain Paths *J. Phys. Conf. Ser.* 896
- [22] Kami A, Dariani B M, Sadough Vanini A, Comsa D S and Banabic D 2015 Numerical determination of the forming limit curves of anisotropic sheet metals using GTN damage model *J. Mater. Process. Technol.* 216 472–83
- [23] Banabic D, Paraianu L, Dragos G, Bichis I and Comsa D S 2009 An improved version of the modified maximum force criterion (MMFC) used for predicting the localized necking in sheet metals *Proc. Rom. Acad. Ser. A - Math. Phys. Tech. Sci. Inf. Sci.* 10 237–43
- [24] Leppin, C, Li, J, Daniel D 2008 Application of a method to correct the effect of non-proportional strain paths on Nakajima test based Forming Limit Curves *Proceedings of the NUMISHEET 2008 Conference* ed P Hora pp 217–21
- [25] Barlat F and Lian K 1989 Plastic behavior and stretchability of sheet metals. Part I: A yield function for orthotropic sheets under plane stress conditions *Int. J. Plast.* 5 51–66